Catalysis Science & Technology

ROYAL SOCIETY OF CHEMISTRY

PAPER

View Article Online
View Journal | View Issue

Cite this: *Catal. Sci. Technol.*, 2025, **15**, 5327

Role of base in CO_2 hydrogenation to formate over a $Ru^{(III)}$ solid micellar catalyst

Catarina M. De Brito Mendes, [a] Javiera Rubio,[a] Francisca Rebelo,[ab] Sara Santos, [a] Jan Öner,[a] Vitaly V. Ordomsky [c] and Mark Saeys *[a]

Received 3rd June 2025,
Accepted 11th August 2025

DOI: 10.1039/d5cy00662g

rsc.li/catalysis

The catalytic conversion of CO_2 to formate is generally performed under basic conditions. While the specific role of amines may not always be clearly defined, they have been the preferred additives to enhance activity and conversion. In this work, we demonstrate that during CO_2 hydrogenation to formate over a $Ru^{(III)}$ solid micellar catalyst, the base acts as a promoter by improving the sluggish heterolytic H_2 dissociation. Kinetic experiments revealed that it is crucial to direct CO_2 speciation towards bicarbonate to ensure formate generation, and that there is a strong dependence of the hydrogenation rate on H_2 and TEA availability. H_2–D_2 isotope scrambling showed a fourfold increase in the presence of the base. Screening of different bases evidenced the unique promoting effect of TEA.

1. Introduction

The catalytic transformation of CO_2 to formate/formic acid is gaining attention due to the potential of formate salts/formic acid for reversible hydrogen storage.[1–3] The synthesis of formic acid from CO_2 and H_2 is endergonic in the gas phase, but the reaction becomes thermodynamically favorable in aqueous medium due to solvation effects.[4,5] Stoichiometric amounts of bases are typically added as co-reagents to promote the stabilization of formic acid as formate salts or adducts.[6] N-containing organic bases, used as reaction additives, and amine-related functional groups, incorporated as ligands in molecular catalysts, promote CO_2 reduction by acting as proton shuttles, capturing CO_2, and providing electronic stabilization to reaction intermediates.[7]

Proton shuttles are important in CO_2 hydrogenation to formate, as they facilitate H_2 heterolytic cleavage into a hydride and a proton. The hydride reacts with CO_2 to produce formate, while the proton needs to be efficiently transferred to a base to close the catalytic cycle. Amines readily accept a proton, forming ammonium. Filonenko *et al.* attributed the high hydrogenation rate over a Ru PNP-pincer catalyst in a mixture of *N*,*N*-dimethylformamide (DMF) and 1,8-diazabicyclo[5.4.0]undec-7-ene (DBU) to the amine-assisted Ru–H bond formation *via* heterolytic dissociation of a coordinated H_2 molecule.[7,8] In their study, activity was further enhanced by increasing H_2 partial pressure. Rawat *et al.* demonstrated that the heterolytic H_2 cleavage and hydride transfer over a series of Fe complexes improved due to the presence of an outer-sphere pendant amine.[9]

Amines have been employed as CO_2 trapping agents in reduction reactions over homogeneous catalysts due to their CO_2-capturing ability.[10] In the presence of water, primary and secondary amines (RNH_2 and R_2NH) react with CO_2 to form carbamates ($RNHCOO^-$ and R_2NCOO^-) which can hydrolyze to produce bicarbonate (HCO_3^-) and protonated amines (RNH_3^+ and $R_2NH_2^+$). Tertiary amines (R_3N) directly form HCO_3^- and protonated tertiary amines (R_3NH^+). In organic solvents, where reactants and products have only one possible form, alkaline aqueous solutions involve multiple equilibria, with reactive species and products varying based on amine type and concentration, pH, temperature and CO_2 partial pressure.[11,12]

High CO_2 conversions have been reported over homogeneous catalysts in the presence of amines, with several examples in the literature displaying advancements in catalyst and process development.[13–15] Compared to homogeneous catalysts, heterogeneous catalysts own several advantages for large-scale application in continuous flow, including improved catalyst stability and lower production costs.[16] Single-site catalysts are especially promising for CO_2 hydrogenation to formate due to their resemblance to homogeneous systems: well-defined active sites, high activity and selectivity.

$Ru^{(III)}$@MCM is the first example of a SOlid MICellar (SOMIC) catalyst, consisting of $Ru^{(III)}$ single sites incorporated into the walls of MCM-41 *via* Ru–O–Si bonds, and stabilized by a cetyltrimethylammonium (CTA^+). The presence of the CTA^+

[a] *Laboratory for Chemical Technology, Department of Materials, Textiles and Chemical Engineering, Ghent University, Technologiepark 125, 9052 Ghent, Belgium. E-mail: mark.saeys@ugent.be*
[b] *Chemical Engineering Department, Instituto Superior Técnico, Universidade de Lisboa, Av. Rovisco Pais, 1049-001 Lisbon, Portugal*
[c] *Univ. Lille, CNRS, Centrale Lille, ENSCL, Univ. Artois, UMR 8181 – UCCS – Unité de Catalyse et Chimie du Solide, F-59000 Lille, France*

molecules prevents sintering and creates an apolar environment in the pores, favoring the concentration of nonpolar reactants and intermediates while excluding bulk water.[17,18] The $Ru^{(III)}$ active sites maintain a local environment where water can still interact through coordination or hydrogen bonding, ensuring their accessibility to aqueous-phase reactants.

At 90 °C and 50 bar, a turnover frequency (TOF) of 182 h^{-1} and a formate concentration of 1 mol L^{-1} after 15 h was reached in aqueous medium and in the presence of TEA over $Ru^{(III)}$@MCM. Catalyst activity and selectivity was maintained over four consecutive CO_2 hydrogenation cycles.[18] DFT modelling suggests that the reaction proceeds *via* heterolytic splitting of H_2, forming a Ru–H species, followed by hydride transfer to CO_2. H_2 activation is the rate-determining step of the reaction and the Ru–H complex is identified as the resting state of the catalyst. The role of base was not explicitly included in the reaction path, but it was hypothesized that the heterolytic H_2 dissociation could happen over $(O)_3SiO^-$, OH^-, HCO_2^-, HCO_3^- or TEA.

In this work, we investigate the reaction kinetics of CO_2 hydrogenation to formate over $Ru^{(III)}$@MCM, focusing on the influence and mechanistic role of the base. Combining the study of the dependence of formate concentration on reaction conditions and H_2–D_2 isotope scrambling, we evaluate the role of pH and CO_2 speciation in the reaction medium, the influence of H_2 partial pressure and TEA concentration on the formate production rate. The performance of a selection of different solvents and bases is evaluated and compared.

2. Experimental

2.1 Chemicals

Hexadecyltrimethylammonium bromide (CTAB, $C_{19}H_{42}BrN$, ≥98%), ruthenium chloride ($RuCl_3$, Ru content 45–55%), ammonium hydroxide solution (NH_4OH, ACS reagent 28–30% NH_3 basis), tetraethyl orthosilicate (TEOS, $SiC_8H_{20}O_4$, reagent grade 98%), triethylamine (TEA, $C_6H_{15}N$, ≥99%), tripropylamine (TPA, $C_9H_{21}N$, ≥98%), triethanolamine (TEOA, $C_6H_{15}NO_3$, ≥98%), *N*,*N*-diisopropylethylamine (DIPEA, $C_8H_{19}N$, ≥99%), propylamine (PA, C_3H_9N, ≥98%), and morpholine (Mor, C_4H_9NO, ≥99%), dimethyl sulfoxide (DMSO, $(CH_3)_2SO$, ≥99%) and methanol (MeOH, CH_3OH, ≥99.8%) were purchased from Merck Chemicals. Ethanol (EtOH, C_2H_5OH, denaturated with Eurodenaturant) was supplied by Chem Lab. Water was deionized using a Millipore system. H_2, CO_2 and Ar were purchased from Air Liquide and D_2 was purchased from Eurisotop. All chemicals were used without further purification.

2.2 Catalyst synthesis

$Ru^{(III)}$@MCM was prepared according to the procedure described by Wang *et al.*[18] 0.5 g of hexadecyltrimethylammonium bromide (CTAB) powder was added to 96 mL of deionized water and 34 mL of ethanol under stirring at 250 rpm for 30 minutes, until a fully transparent solution was obtained. Then, 0.09 g of ruthenium(III) chloride was added to the mixture and stirred at 650 rpm for 20 minutes to ensure $RuCl_3$ was fully dissolved. Next, 10 mL of aqueous ammonium hydroxide solution (NH_4OH) was added, followed by the dropwise addition of 2 mL of tetraethyl orthosilicate (TEOS). The resulting solution was stirred for three hours at room temperature. Approximately 1 g of solid product was collected through vacuum filtration, washed with distilled water until the filtrate attained a neutral pH, and finally dried overnight at room temperature.

$Ru^{(III)}$@Mic is the homogeneous counterpart of $Ru^{(III)}$@MCM. 0.5 g of CTAB powder was added to 96 mL of deionized water and 34 mL of ethanol. The mixture was stirred at 250 rpm for 30 minutes until a fully transparent solution was obtained. Then, 0.09 g of ruthenium(III) chloride was added to the mixture and stirred at 650 rpm for 20 minutes, ensuring complete dissolution of $RuCl_3$. No TEOS was introduced.

2.3 Catalytic tests

Hydrogenation reactions were performed in a 45 mL stainless steel pressure reactor manufactured by Parr Instrument Company, with a PTFE inner chamber. During reaction, the vessel was placed in an aluminum support placed on a ceramic hot plate stirrer (IKA C-MAG HS7). Temperature was controlled using an electronic contact thermometer (IKA ETS-D5) placed in the aluminum support (Fig. S1, SI).

In a standard procedure, the vessel was initially filled with water, base, fresh catalyst and a magnetic stirrer. Then, the reactor was sealed, purged with CO_2, pressurized with the gaseous reactants and gradually heated to the desired reaction temperature for 30 minutes. After reaction, the vessel was cooled to room temperature, the pressure released and the gas phase analyzed *via* gas chromatography (GC). The liquid product was separated from the catalyst using a syringe filter. Quantitative analysis of the formate concentration in the liquid product (C_{HCOO^-}) was performed *via* ^1H NMR using a Spinsolve 80 MHz phosphorous benchtop NMR spectrometer from Magritek and TSP-d_4 as internal standard (Fig. S2, SI). The standard deviation was calculated based on eqn (1), in which $C_{HCOO^-,i}$ is the individual formate concentration measured from each sample, $\overline{C_{HCOO^-}}$ is the average of the concentrations measured for each reaction and n is the total number of measurements.

$$\text{Standard deviation} = \sqrt{\frac{\sum \left(C_{HCOO^-,i} - \overline{C_{HCOO^-}}\right)^2}{(n-1)}} \quad (1)$$

The turnover frequency (TOF) and base conversion were calculated as defined in eqn (2) and (3), respectively.

$$\text{TOF}\ (h^{-1}) = \frac{C_{HCOO^-} \times V}{n_{Ru} \times t} \quad (2)$$

$$X_{base}\ (\%) = \frac{n_{HCOO^-}}{n^0_{base}} \quad (3)$$

where V is the volume of the reaction product, n_{Ru} is the amount of Ru (mol) in the catalyst used, t is the reaction time

(h), n_{HCOO^-} is the amount of formate (mol) in the reaction product, and n^0_{base} is the amount of base (mol) added to the reaction feed.

2.4 H_2–D_2 isotope scrambling

H_2–D_2 exchange reactions were performed using the same autoclave employed for the catalytic tests. Prior to each reaction, water, base and fresh catalyst were added to the autoclave. The reactor was sealed, pressurized with H_2 and D_2 with a ratio 1 : 1, and heated to the reaction temperature for 15 min. After reaction, the vessel was cooled to room temperature and connected to a mass spectrometer (MS) for off-line gas analysis. The gas released from the reactor was continuously diluted with argon (Ar) as a carrier gas in a flow line, ensuring a flow rate of 50 Nml min^{-1}. This diluted gas mixture was analyzed using Mass Spectrometry (MS) to monitor the composition until all the gas content was released from the autoclave. During the analysis, the relative intensities of H_2, D_2, and HD were quantified by calculating the signal ratios H_2/Ar, D_2/Ar, and HD/Ar. These ratios were derived from the raw MS signals recorded throughout the analysis period, providing a comparative measure of each gas component relative to the inert Ar reference.

3. Results and discussion

3.1 Kinetic insights

The effect of reaction time on formate concentration, catalyst activity, and TEA conversion was evaluated in a range from 3 to 20 h. The maximum formate concentration reached is 1.23 mol L^{-1} after 20 h (Table 1, entry 6), aligning with the catalyst performance previously reported.[18] Gas chromatography analysis confirmed the absence of CO and CH_4 after reaction. Catalyst productivity peaks at 2.6 g $HCOO^-$ per $g_{cat.}$ h^{-1} (TOF = 214 h^{-1}) after 10 h (Table 1, entry 4). The pH remains constant throughout the reaction, and formate production increases linearly during the first ten hours. As the reaction progresses, activity slows down at formate concentrations higher than 1 mol L^{-1} (Table 1, entries 4 to 6), near full TEA conversion. To guarantee the collection of kinetic data throughout our study, a reaction time of 4 h (X_{TEA} ~ 24%, Table 1) was selected to study the dependence of formate concentration on the reaction conditions.

Table 1 Effect of reaction time on formate concentration, catalyst activity and TEA conversion. Conditions: 3.1 μmol Ru, 9 mmol TEA, 6 mL H_2O, 30 bar H_2, 20 bar CO_2, 90 °C

Entry	Reaction time (h)	[$HCOO^-$] (mol L^{-1})	TOF (h^1)	X_{TEA} (%)
1	3	0.08	56	5.9
2	4	0.31	158	24.2
3	5	0.42	174	30.5
4	10	1.03	214	75.9
5	15	1.09	162	85.4
6	20	1.23	137	95.8

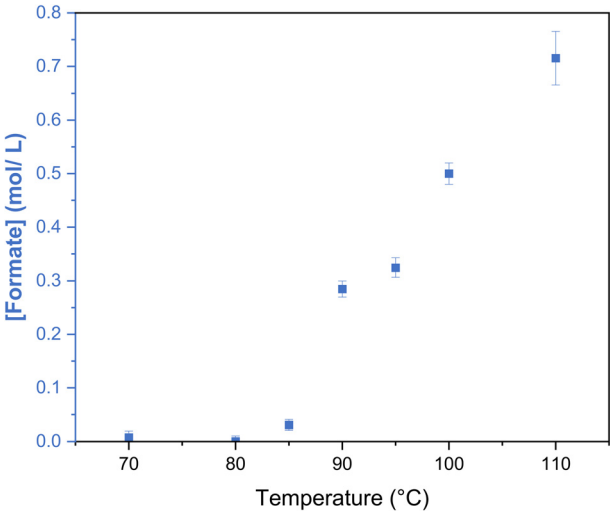

Fig. 1 Effect of temperature on formate concentration. Conditions: 3.1 μmol Ru, 9 mmol TEA, 6 mL H_2O, 30 bar H_2, 20 bar CO_2, 4 h.

The catalytic hydrogenation of CO_2 over $Ru^{(III)}$@MCM in the liquid phase requires the transfer of CO_2 and H_2 from the gas to the liquid phase, from the liquid phase to the external surface of the catalyst and finally to and within the pores of the catalyst. A study of the effect of stirring speed indicates no external mass transfer limitations above 750 rpm (Fig. S3, SI).

Varying the reaction temperature from 70 to 110 °C (Fig. 1) showed that formate production becomes measurable at 85 °C, and that an increase in the temperature improves CO_2 hydrogenation. The apparent activation energy (E_{app}) is 56 kJ mol^{-1} (Fig. S4, SI).

The dependence of formate concentration on the gaseous reactants partial pressure was investigated. A limited effect of CO_2 partial pressure is found (Fig. S5, SI). In contrast, there is a significant influence of H_2 partial pressure on the product concentration. An increase from to 10 to 30 bar leads to a tenfold increase of formate concentration (0.31 mol L^{-1}, Fig. 2) in the reaction product. A quasi-second order in H_2 is calculated (Fig. S6, SI), indicating that H_2 adsorption and activation are kinetically relevant.

The reaction was also studied at different TEA concentrations in the feed (X_{TEA} < 25%). In water, a very low concentration of formic acid is obtained (Fig. S7, SI). Formate concentration increases linearly from 0.05 to 0.35 mol L^{-1} when the TEA concentration in the aqueous reaction feed is varied from 0.6 to 1.5 mol L^{-1} (Fig. 3), all at low TEA conversion (X_{TEA} < 25%). When the concentration of TEA in the reaction feed exceeds 1.5 mol L^{-1}, catalyst performance drops (Fig. 3). Extending the reaction time from 4 h to 15 h shows a similar effect (Fig. S8, SI).

The decrease in the $Ru^{(III)}$@MCM performance at higher TEA concentrations can be linked to a change in the pH of the liquid phase. Within the pH range of 8–9, bicarbonate (HCO_3^-) is the main form of carbon in solution (Fig. S9, SI). In a more alkaline medium, carbonate (CO_3^{2-}) becomes the dominant

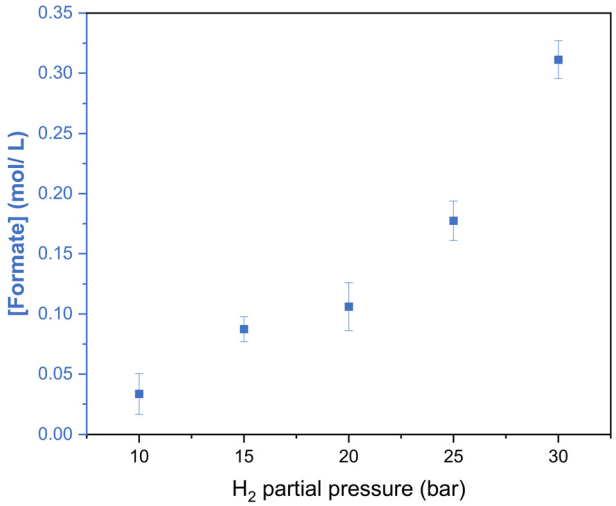

Fig. 2 Dependence of the formate concentration on H_2 partial pressure. Conditions: 3.1 μmol Ru, 9 mmol TEA, 6 mL H_2O, 20 bar CO_2, 90 °C, 4 h.

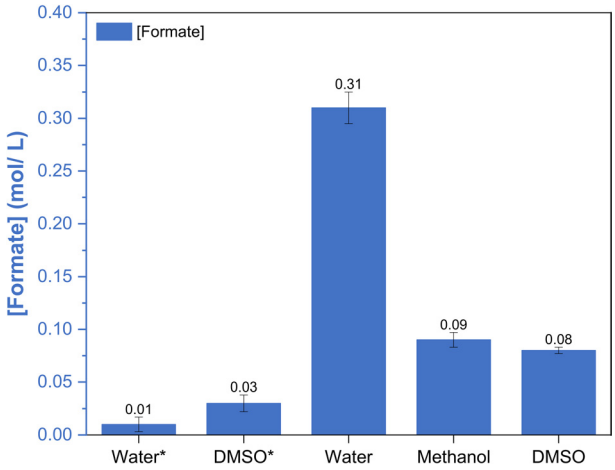

Fig. 4 Performance of $Ru^{(III)}$@MCM for CO_2 hydrogenation to formic acid/formate in different solvents. Conditions: 3.1 μmol Ru, no TEA* or 9 mmol, 6 mL solvent, 30 bar H_2, 20 bar CO_2, 90 °C, 4 h.

species (Fig. S9, SI). $KHCO_3$ was directly hydrogenated at pH 12 in the absence of CO_2 (entry 2, Table S1, SI, Fig. S10, SI), resulting in no formate production. However, when $KHCO_3$ hydrogenation was performed under CO_2 pressure at pH 8 (entry 4, Table S1, SI, Fig. S11, SI), the formate concentration increased significantly, surpassing that of the standard TEA-based system (0.31 mol L^{-1}, entry 1, Table S1, SI). In contrast, performing CO_2 hydrogenation at pH 8 in the presence of $KHCO_3$ but without TEA led to a notably lower formate concentration (entry 5, Table S1, SI, Fig. S12, SI), indicating that maintaining the pH at 8 alone is insufficient for high catalytic activity. Direct hydrogenation of K_2CO_3 at pH 13 (entries 6 to 8, Table S1, SI, Fig. S13 and S14, SI) does not yield formate. CO_2 hydrogenation in the presence of K_2CO_3 generates 0.26 mol L^{-1} of formate (entry 9, Table S1, SI, Fig. S15, SI), highlighting that K_2CO_3 can serve as a base in the reaction.

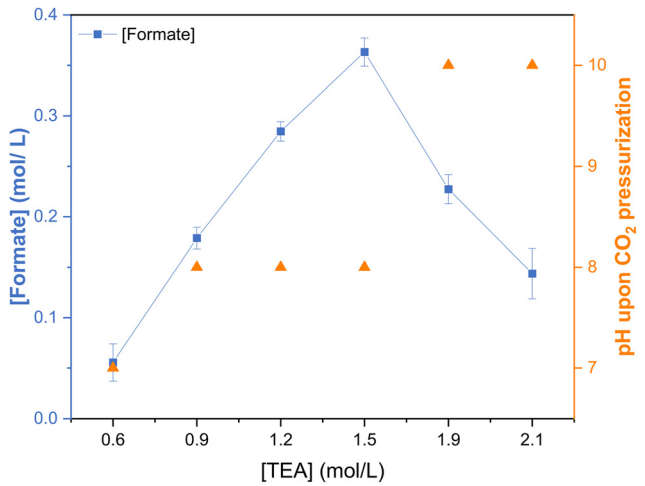

Fig. 3 Dependence of the formate concentration on the amount of TEA in the liquid reaction feed and pH upon CO_2 pressurization. Conditions: 3.1 μmol Ru, 6 mL H_2O, 30 bar H_2, 20 bar CO_2, 90 °C, 4 h.

These results suggest that at high TEA concentration or during the direct hydrogenation of $KHCO_3$ and K_2CO_3 the reaction does not proceed because the alkalinity of the medium favors the formation of CO_3^{2-} over HCO_3^-. In the presence of CO_2, the pH decreases (Fig. 3, Table S2, SI), shifting the equilibrium towards HCO_3^-. Keeping the pH of the reaction medium in the range 8–9 to maintain HCO_3^- as the predominant species in solution seems crucial for formate synthesis over $Ru^{(III)}$@MCM (Fig. 3).

As the choice of solvent can impact both the reaction thermodynamics and catalytic mechanism,[19] CO_2 hydrogenation over $Ru^{(III)}$@MCM was further studied in DMSO and in methanol (Table S3, SI). Fig. 4 shows that in the absence of a base, the performance of $Ru^{(III)}$@MCM in DMSO is similar to the one observed in water. The group of Leitner reported that DMSO stabilizes HCOOH by hydrogen bonding.[6] Our results demonstrate that replacing water and TEA by a solvent to promote formic acid stabilization did not lead to a higher formate concentration in our system (Fig. 4). Performing the reaction in MeOH and DMSO in the presence of TEA generated formate concentrations three times lower (approximately 0.1 mol L^{-1}) than in aqueous medium (Fig. 4). Similarly, gradually increasing the amount of MeOH and DMSO in mixtures with water did not lead to improved performance (Tables S4 and S5, SI). In aqueous environments, TEA reacts with CO_2 to produce HCO_3^-. In non-aqueous solvents such as methanol or DMSO, CO_2 interaction with tertiary amines is limited.[20]

3.2 Role of the base

The quasi-second order in H_2 (Fig. S6, SI) and the first order in TEA concentration (Fig. 3) suggest that the tertiary amine is involved in H_2 activation. To investigate the involvement of TEA in the heterolytic H_2 cleavage step during the CO_2 hydrogenation to formate, a set of three H_2–D_2 isotope scrambling experiments was carried out (Table 2). H_2–D_2 scrambling involves exposing hydrogen molecules to a

Table 2 Summary of reaction conditions for H_2–D_2 isotope scrambling experiments and ratios between the MS raw signals of H_2, D_2, HD and Ar after reaction. Reaction conditions: 4 bar H_2, 4 bar D_2, 1 mL H_2O, 50 °C, 1 h, analysis conditions: total flow of 50 mL min^{-1} fed to the MS (90% Ar)

Entry	Ru (μmol)	TEA (mmol)	Ratio of the MS signals		
			H_2/Ar	D_2/Ar	HD/Ar
1	0	0	0.59	0.19	0.01
2	3.1	0	0.60	0.17	0.08
3	3.1	1.4	0.28	0.10	0.30

catalyst under specific conditions, allowing for the exchange of hydrogen atoms with deuterium atoms. Breaking of H–H bonds and the incorporation of deuterium atoms leads to the appearance of HD as a reaction product. By monitoring the extent of HD in the reaction products, conclusions about the catalyst's capacity to dissociate H_2 can be drawn as well as the involvement of the base.

Fig. S16, SI shows the mass spectrometer signals of H_2, D_2, HD and H_2O during the off-line analysis of the autoclave gas content, after dilution in Ar. In the absence of both the catalyst and base, only a negligible amount of HD is formed (Table 2, entry 1). Introducing $Ru^{(III)}$@MCM (Table 2, entry 2) results in an eightfold increase in the HD/Ar ratio, demonstrating the catalyst's critical role in activating H_2 and facilitating hydrogenation. When TEA is added to the system (Table 2, entry 3), the HD/Ar ratio increases another fourfold. The combined presence of $Ru^{(III)}$@MCM and TEA creates a synergistic effect, significantly boosting HD production and supporting the hypothesis that the base modifies the reaction mechanism.

To further confirm the involvement of TEA in H_2 dissociation, ^{1}H NMR spectroscopy was conducted using the homogeneous parent complex of the Ru SOMIC catalyst, $Ru^{(III)}$@Mic. Upon pressurization with H_2 and heating at 50 °C for 1.5 hours, distinct changes were observed in the chemical shifts of TEA (Fig. S17, SI (d)) compared to control samples lacking H_2 (Fig. S17, SI (c)) or $Ru^{(III)}$@Mic (Fig. S17, SI (e) and (f)). Notably, the CH_2 resonance of TEA shifted downfield from 2.53 ppm (Fig. S17, SI (c)) to 2.78 ppm under reaction conditions (Fig. S17, SI (d)), indicating a change in the electronic environment around the nitrogen atom consistent with protonation.[21]

The proposed pathway for CO_2 hydrogenation in the presence of TEA is illustrated in Fig. 5. The first step concerns H_2 adsorption on the Ru active center. The formation of intermediate 2 (**Int 2**) is followed by TEA-assisted H_2 heterolytic dissociation *via* transition state 1 (**TS 1**), leading to the generation of a Ru hydride species and triethylammonium (**Int 3**). In the next step, the hydride is transferred to CO_2 (**TS 2**), which exists in dynamic equilibrium with HCO_3^- under basic conditions. The catalytic cycle is closed by formate (**Int 4**) removal from the active site aided by triethylammonium.

The reaction involves the transport of key components—H_2, CO_2, and the amine—through the apolar medium formed by the CTA^+ surfactant within the pores of the $Ru^{(III)}$@MCM structure. The apolar environment within these pores plays a critical role in mediating the interaction of the reactants with the catalytic active sites. Effective base-mediated catalysis depends on the amine's basicity and ability to partition into the nonpolar pore environment, and subsequently interact with the

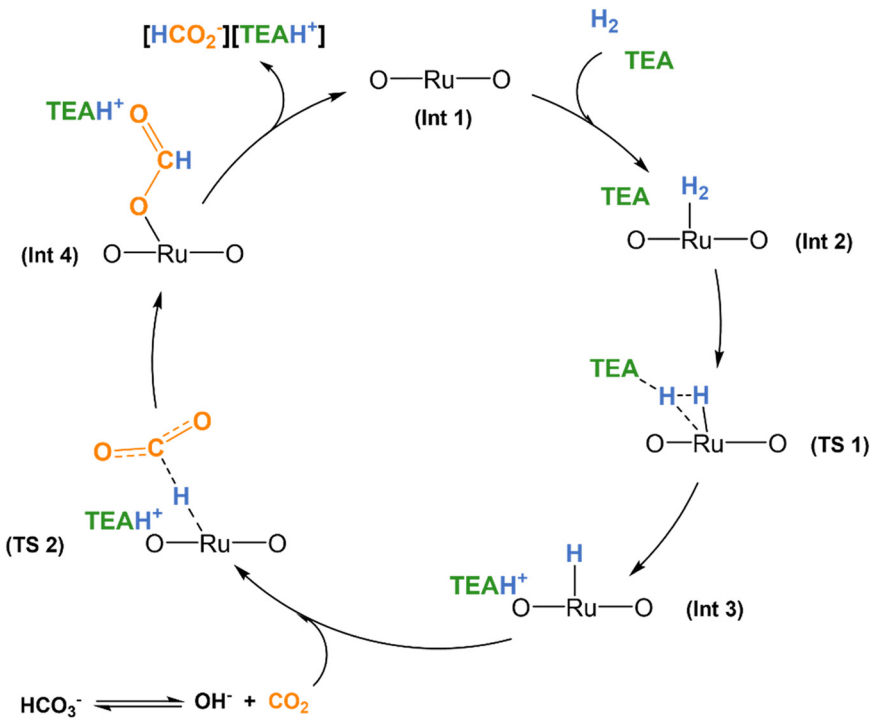

Fig. 5 A proposed mechanism for formate synthesis over $Ru^{(III)}$@MCM in the presence of TEA.

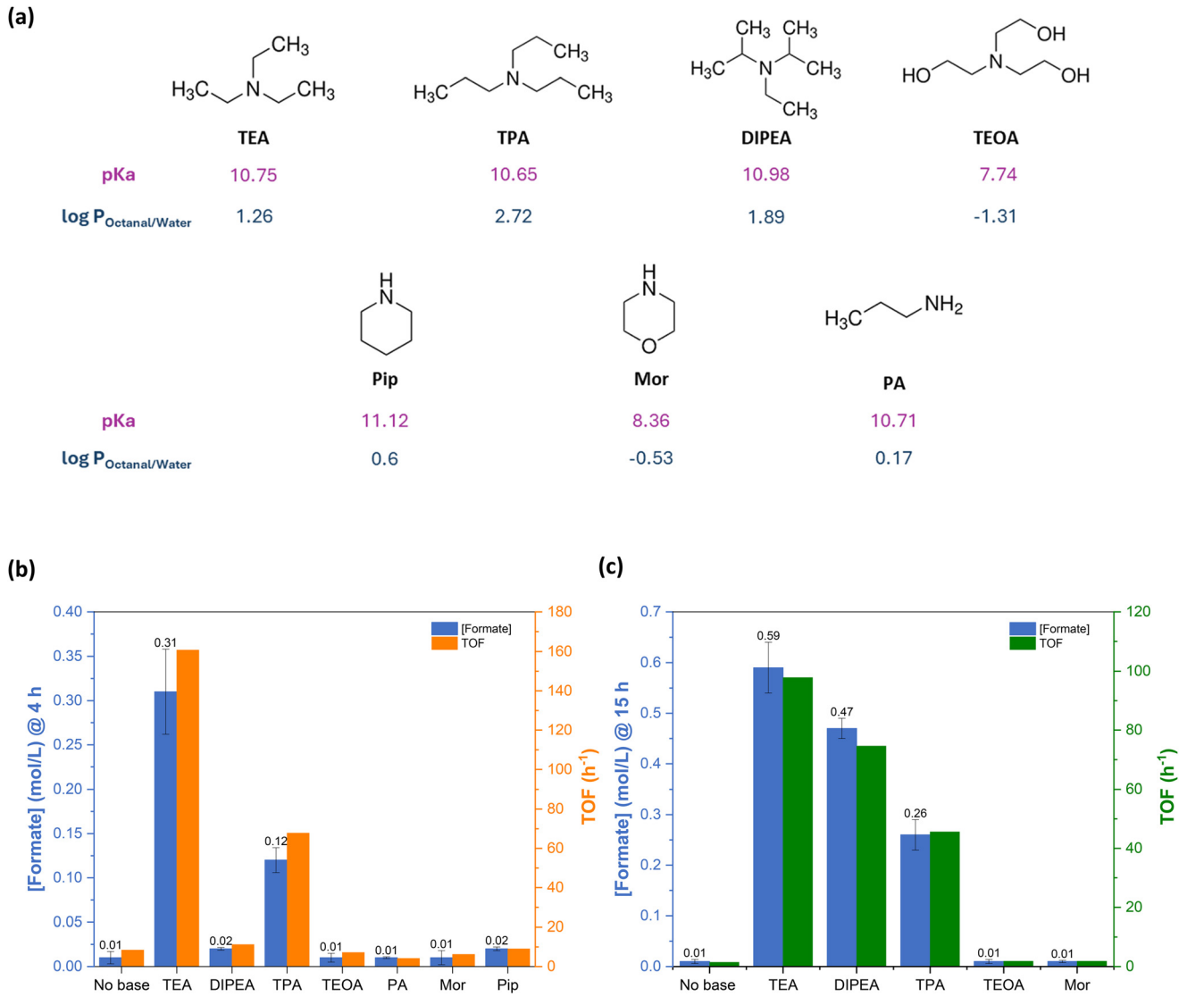

Fig. 6 Screening of amines with different basicity and lipophilicity. (a) for CO_2 hydrogenation to formate over $Ru^{(III)}$@MCM (b) and $Ru^{(III)}$@Mic (c). Conditions: 3.1 μmol Ru, 9 mmol of amine, 4.5 mmol EtOH (b), 6 mL H_2O, 30 bar H_2, 20 bar CO_2, 90 °C, 4 h (b) or 15 h (c).

metal site. Different tertiary, secondary and primary amines with varied basicity, lipophilic and steric properties (Table S6, SI, Fig. 6(a)) were screened for CO_2 hydrogenation over $Ru^{(III)}$@MCM, and their performance compared to that of TEA (Fig. 6(b)). Lipophilicity was evaluated based on the partition coefficient between *n*-octanal and water ($\log P_{Octanal/Water}$), chosen as a model system to mimic the hydrophobic environment within the pores of $Ru^{(III)}$@MCM and the aqueous phase.

TEA combines high basicity (pK_a = 10.75), moderate lipophilicity ($\log P_{Octanal/Water}$ = 1.26), and low steric hindrance, and consequently exhibited the strongest promoting effect on formate production among all amines tested (Fig. 6(b)). TPA has a similar basicity to TEA and is more lipophilic ($\log P_{Octanal/Water}$ = 2.72), but its bulkier alkyl chains likely hinder diffusion or orientation within the confined pore environment, resulting in approximately 3-fold lower activity. Interestingly, while both DIPEA and TEOA are tertiary amines, they were nearly inactive, comparable to the control reaction without base. This highlights that tertiary structure alone is not sufficient for promotion. DIPEA is strongly basic (pK_a = 10.98) and fairly lipophilic ($\log P_{Octanal/Water}$ = 1.89), but its significant steric bulk —arising from branched isopropyl groups—likely hinders its diffusion through the catalyst pores, resulting in poor performance. In contrast, TEOA has lower basicity (pK_a = 7.74) and is highly hydrophilic ($\log P_{Octanal/Water}$ = −1.31), though it is small and sterically unhindered. These findings indicate that an optimal combination of strong basicity, intermediate lipophilicity, and minimal steric hindrance is essential to facilitate efficient base promotion within this catalytic system.

To evaluate to which extent poor pore accessibility as result of the bulkier nature of DIPEA might influence formate production, the same tertiary amines were screened over $Ru^{(III)}$@Mic (Fig. 6(c)). In these conditions, DIPEA outperformed TPA.

The higher TOF of $Ru^{(III)}$@MCM compared to $Ru^{(III)}$@Mic can be a result of the increased electron density around the metal ion, promoted by the interaction with the supporting silica matrix.

Finally, screening secondary and primary amines, within the same range of pK_a,[8–11] led to productivities ten to twenty times lower than tertiary amines. Since secondary and primary amines typically react with CO_2 to form stable carbamates, we hypothesize these species are less reactive over $Ru^{(III)}$@MCM.

4. Conclusions

The study of the liquid phase kinetics of CO_2 hydrogenation to formate over $Ru^{(III)}$@MCM provides a deeper understanding of the reaction's dependence on H_2 partial pressure, concentration of TEA, pH, choice of solvent and role of the base.

The observed quasi second-order dependence in H_2 partial pressure reveals the importance of hydrogen activation for the reaction. High initial concentrations of TEA prevent the reaction because the high alkalinity of the medium favors formation of CO_3^{2-} over HCO_3^-. Performing the reaction in water guarantees HCO_3^- formation over carbamates and maintaining a pH between 8–9 is crucial to keep HCO_3^- as the predominant species, ensuring formate synthesis over $Ru^{(III)}$@MCM.

H_2–D_2 isotope scrambling confirms that the catalyst is able to activate H_2, with the addition of a TEA significantly enhancing formate production. Among the amines screened, TEA has the highest promoting effect. The presence of a base in the vicinity of the $Ru^{(III)}$ active centers is crucial for H_2 heterolytic dissociation during reaction. Small bases, with a moderate lipophilicity and a pK_a above 10 are preferred as promoters.

These findings provide insights into the role of bases in CO_2 hydrogenation over $Ru^{(III)}$@MCM and guide optimization strategies for selective, base-free formic acid synthesis.

Author contributions

Catarina M. De Brito Mendes: conceptualization, investigation, formal analysis, validation, visualization, writing – original draft, writing – review and editing. Javiera Rubio: investigation. Francisca Rebelo: investigation. Sara Santos: investigation. Jan Öner: writing – review and editing. Vitaly V. Ordomsky: writing – review and editing. Mark Saeys: conceptualization, funding acquisition, project administration, supervision, writing – review & editing.

Conflicts of interest

There are no conflicts of interest to declare.

Data availability

Supplementary information is available. See DOI: **https://doi.org/10.1039/D5CY00662G**.

The processed data supporting this article (^{1}H NMR and MS) has been included as part of the SI. Raw data are available on request from the corresponding author.

Acknowledgements

This research was supported by the Energy Transition Fund, an initiative from the Belgian FPS Economy, under the Molecules at Sea (MuSE) project. The author V. V. O. acknowledges the financial support of the French National Research Agency (DEZECO, Ref. ANR-22- CE05-0005).

References

1 J. Eppinger and K.-W. Huang, Formic Acid as a Hydrogen Energy Carrier, *ACS Energy Lett.*, 2017, **2**(1), 188–195.
2 K. Grubel, H. Jeong, C. W. Yoon and T. Autrey, Challenges and opportunities for using formate to store, transport, and use hydrogen, *J. Energy Chem.*, 2020, **41**, 216–224.
3 S. Chatterjee, I. Dutta, Y. Lum, Z. Lai and K.-W. Huang, Enabling storage and utilization of low-carbon electricity: power to formic acid, *Energy Environ. Sci.*, 2021, **14**(3), 1194–1246.
4 W. Leitner, Carbon dioxide as a raw material: the synthesis of formic acid and its derivatives from CO_2, *Angew. Chem., Int. Ed. Engl.*, 1995, **34**(20), 2207–2221.
5 R. Sun, Y. Liao, S.-T. Bai, M. Zheng, C. Zhou and T. Zhang, *et al.*, Heterogeneous catalysts for CO_2 hydrogenation to formic acid/formate: from nanoscale to single atom, *Energy Environ. Sci.*, 2021, **14**(3), 1247–1285.
6 K. Rohmann, J. Kothe, M. W. Haenel, U. Englert, M. Hölscher and W. Leitner, Hydrogenation of CO_2 to Formic Acid with a Highly Active Ruthenium Acriphos Complex in DMSO and DMSO/Water, *Angew. Chem., Int. Ed.*, 2016, **55**(31), 8966–8969.
7 J. B. Jakobsen, M. H. Rønne, K. Daasbjerg and T. Skrydstrup, Are Amines the Holy Grail for Facilitating CO_2 Reduction?, *Angew. Chem., Int. Ed.*, 2021, **60**(17), 9174–9179.
8 G. A. Filonenko, R. van Putten, E. N. Schulpen, E. J. M. Hensen and E. A. Pidko, Highly Efficient Reversible Hydrogenation of Carbon Dioxide to Formates Using a Ruthenium PNP-Pincer Catalyst, *ChemCatChem*, 2014, **6**(6), 1526–1530.
9 K. S. Rawat, A. Mahata and B. Pathak, Catalytic Hydrogenation of CO_2 by Fe Complexes Containing Pendant Amines: Role of Water and Base, *J. Phys. Chem. C*, 2016, **120**(47), 26652–26662.
10 R. E. Siegel, S. Pattanayak and L. A. Berben, Reactive Capture of CO_2: Opportunities and Challenges, *ACS Catal.*, 2023, **13**(1), 766–784.
11 G. Kovács, G. Schubert, F. Joó and I. Pápai, Theoretical investigation of catalytic $HCO3^-$ hydrogenation in aqueous solutions, *Catal. Today*, 2006, **115**(1), 53–60.
12 R. Zhang, R. Liu, F. Barzagli, M. G. Sanku, L. Ce and M. Xiao, CO_2 absorption in blended amine solvent: Speciation, equilibrium solubility and excessive property, *Chem. Eng. J.*, 2023, **466**, 143279.
13 J. Kothandaraman, A. Goeppert, M. Czaun, G. A. Olah and G. K. Surya Prakash, CO_2 capture by amines in aqueous media and its subsequent conversion to formate with

reusable ruthenium and iron catalysts, *Green Chem.*, 2016, **18**(21), 5831–5838.

14 T. Schaub and R. A. Paciello, A process for the synthesis of formic acid by CO_2 hydrogenation: thermodynamic aspects and the role of CO, *Angew. Chem., Int. Ed.*, 2011, **32**(50), 7278–7282.

15 K. R. Ehmann, A. Nisters, A. J. Vorholt and W. Leitner, Carbon Dioxide Hydrogenation to Formic Acid with Self-Separating Product and Recyclable Catalyst Phase, *ChemCatChem*, 2022, **14**(19), e202200892.

16 C. Kim, K. Park, H. Lee, J. Im, D. Ususky and K. Tak, *et al.*, Accelerating the net-zero economy with CO2-hydrogenated formic acid production: Process development and pilot plant demonstration, *Joule*, 2024, **8**(3), 693–713.

17 Q. Wang, C. M. De Brito Mendes, O. V. Safonova, W. Baaziz, C. A. Urbina-Blanco and D. Wu, *et al.*, Tunable catalysis by reversible switching between $Ru^{(III)}$ single sites and Ru^0 clusters in solid micelles, *J. Catal.*, 2023, **426**, 336–344.

18 Q. Wang, S. Santos, C. A. Urbina-Blanco, W. Y. Hernández, M. Impéror-Clerc and E. I. Vovk, *et al.*, Solid micellar Ru single-atom catalysts for the water-free hydrogenation of CO_2 to formic acid, *Appl. Catal., A*, 2021, **290**, 120036.

19 S. A. Burgess, A. M. Appel, J. C. Linehan and E. S. Wiedner, Changing the Mechanism for CO_2 Hydrogenation Using Solvent-Dependent Thermodynamics, *Angew. Chem., Int. Ed.*, 2017, **56**(47), 15002–15005.

20 L. B. Hamdy, C. Goel, J. A. Rudd, A. R. Barron and E. Andreoli, The application of amine-based materials for carbon capture and utilisation: an overarching view, *Mater. Adv.*, 2021, **2**(18), 5843–5880.

21 D. B. G. Berry, I. Clegg, A. Codina, C. L. Lyall, J. P. Lowe and U. Hintermair, Convenient and accurate insight into solution-phase equilibria from FlowNMR titrations, *React. Chem. Eng.*, 2022, **7**(9), 2009–2024.